

# Computational Flow Optimization of Rotary Blood Pump Components

James F. Antaki, \*Omar Ghattas, Greg W. Burgreen, and \*Beichang He

*University of Pittsburgh, Artificial Heart and Lung Program, and \*Computational Mechanics Laboratory, Department of Civil Engineering, Carnegie Mellon University, Pittsburgh, Pennsylvania, U.S.A.*

---

**Abstract:** In an effort to improve and automate the fluid dynamic design of rotary blood pumps, a coupled computational fluid dynamics (CFD) shape optimization methodology has been developed and implemented. This program couples a finite element flow simulation with a gradient-based optimization routine to modify automatically the shape of an initial candidate blood path, according to a variety of desired fluid dynamic criteria, including shear stress, vorticity/circulation, and viscous dissipation. Preliminary results have led to both intuitive and nonintuitive transformations of the initial blood flow

paths for both internal and external flows. This application of computer design optimization offers the ability to explore a much broader design space much more efficiently than would be possible with traditional parametric methods. It is believed that this computer tool can assist developers of rotary blood pumps in designing blood-wetted components that minimize thrombosis and hemolysis while simultaneously providing maximum flow performance. **Key Words:** Computational fluid dynamics—Design optimization—Shape optimization—Blood trauma—Artificial organs—Mathematical models.

---

The desire to develop a rotary blood pump that simultaneously satisfies the competing requirements of satisfactory hydrodynamic performance, minimal shear versus exposure time, minimal acceleration forces, absence of cavitation, acceptable physical size, and maximum efficiency leads to a challenging problem in design optimization. The conventional design process used in blood pump development has traditionally relied heavily on parametric empirical analyses and trial-and-error methods. The process of fine tuning many design parameters is a time-intensive and laborious process, and the successes achieved to date indeed bear testimony to the ingenuity and persistence of the innovators in this field. However, future efforts to redesign these devices or to develop new devices for different applications will necessitate repetition of the entire arduous empirical process. In addition to its cost and inefficiency, this approach cannot guarantee the best possible final design.

Advanced computational methods, such as computational fluid dynamics (CFD), offer an opportunity to partially facilitate this design process. They can permit novel conceptual designs to be explored and evaluated prior to expensive prototyping and in vitro testing. However, for these techniques to receive practical application as a design tool in the early stages of blood pump development, further advances will be needed on at least three key fronts: improved models to describe the governing physics of blood flow, improved criteria for relating the bulk phenomena of performance and biocompatibility to the microscopic features of the flow, and automated algorithms for updating and refining the design based on microflow features identified (1,2). The focus of the current work is to address these requirements by coupling computerized numerical optimization with CFD analysis into an integrated flow optimization methodology.

Research in aerodynamic design has been similarly motivated to couple CFD with numerical optimization to supplement empirical design (e.g., items one and two from the above list), thus partially automating the design process. The extension of this concept to blood flow, however, has yet to

---

Received March 1995.

Address correspondence and reprint requests to Dr. James F. Antaki, University of Pittsburgh, Artificial Heart and Lung Program, C-826 Presbyterian Hospital, Pittsburgh, PA 15213, U.S.A.

be accomplished. This paper describes the initial development and implementation of such a coupled methodology, specifically intended to evolve flow-optimized blood-wetted components of rotary blood pumps. This program integrates a finite element flow simulation with a gradient-based optimization routine to modify automatically the shape of initial candidate blood paths, according to a desired index of performance, or "objective function." This program provides the option for selecting combinations of objective functions from a variety of fluid dynamic parameters which may directly and indirectly cause blood damage, such as shear stress, vorticity/circulation, and viscous dissipation.

## MATERIALS AND METHODS

### Formulation of the optimization problem

The general application of a rigorous theory of mathematical optimization to the design of a rotary blood pump system requires the identification of the following ingredients: an appropriate index of performance, or "objective function"; a set of design parameters that define the design; a mathematical model, or simulation, to predict performance for a given set of parameters; and a means for adjusting the parameters to improve the performance.

This general description of the problem may encompass a wide range of features of the blood pump design. The concentration of this current study, however, is restricted to the optimization of the shape, or geometry, of a flow path to minimize blood cell trauma and thrombosis. Accordingly, the choice of objective function, design parameters, and system model must be chosen to reflect these aims. These are described in the following sections.

### Objective function selection

It is generally accepted that the critical flow-related concerns in rotary pump design are to maximize hydrodynamic performance while avoiding adverse treatment of the blood elements. Serendipitously, flow features responsible for biocompatibility should also promote good hydrodynamic performance. However, the converse is not necessarily true (3).

Numerous basic experimental studies have demonstrated that high stress levels can result in direct or delayed destruction of blood cells (4-7). As a result, flow conditions leading to turbulence, jet formation, cavitation, and rapid acceleration should be avoided. Additionally, regions of retarded flow—zones of recirculation and stagnation—have been demonstrated to bear strong correlation with the

deposition of blood elements within prosthetic devices (8,9). The combination of elevated shear followed by separated flow delivers a particularly pernicious "one-two punch" (10) with respect to thrombus formation. In such flow fields, platelets are activated by shear exposure and subsequently introduced into a low shear environment in which they are free to form platelet aggregates or attach to adsorbed proteins on the biomaterial surface. Recirculation zones or wakes following a flow separation point (e.g., at the trailing edge of an impeller blade) can further exacerbate blood damage and thrombosis since cells entrapped within them may be exposed to higher concentrations of platelet agonists for extended periods.

Based on this collective evidence, it can be surmised that design optimization of blood-wetted components should seek to minimize shear stress versus exposure time, boundary layer separation leading to zones of stagnation and recirculation, turbulence, excessive particle accelerations, and negative pressures leading to cavitation. In the current work, three principal fluid dynamic objective functions were investigated that may directly or indirectly relate to these adverse phenomena. These are integral of principal shear stress over the domain,  $\Omega$ :

$$f_1 = \int_{\Omega} \tau_v dV \quad (1)$$

integral of vorticity magnitude

$$f_2 = \int_{\Omega} \|\nabla \times v\| dV \quad (2)$$

and index of viscous energy dissipation rate:

$$f_3 = \Phi = \int_{\Omega} \frac{1}{2} D:D dV \quad (3)$$

Here,  $v$  is the vector quantity representing the three components of velocity, and  $D$  is the strain rate tensor equal to  $\frac{1}{2}[(\text{grad } v) + (\text{grad } v)^T]$ . The latter integral quantity represents the viscous energy dissipated over the domain of the flow field; thus, it directly relates to efficiency and indirectly relates to viscous heating, both undesirable conditions with respect to blood damage. The function involving vorticity is intended to indirectly indicate the presence and magnitude of any recirculation bubbles that may be present in the flow. The integral of shear is considered as a more direct indicator of global blood damage, but it is likely to preferentially reflect flow within boundary layers or "hot spots" within the flow field. Each of these objective

functions was studied independently, normalized to the area or volume of the domain, and in linear combination.

#### System model—CFD solver

For the purposes of this initial study, the flow of blood was assumed to be governed by the incompressible Navier-Stokes and conservation of mass equations:

$$\rho \frac{Dv}{Dt} = -\text{grad}(p) + \text{div}(2\mu D)$$

$$\text{div}(v) = 0$$

Here,  $\rho$  is the fluid density (1.03 g/cc), and  $\mu$  is the fluid viscosity. The latter is characterized for normal blood by an asymptotic viscosity,  $\mu$  equals  $\mu_\infty$  equals 3.3 cPs. Use of this equation assumes that blood can be treated as a single-phase homogeneous linearly viscous fluid.

Since the flow equations defined over complex passages typically found within rotary blood pumps do not readily lend themselves to a closed-form solution, a numerical approximation of the flow field was sought, thus enabling calculation of the objective functions. A Galerkin finite-element program, tailored to shape optimization, was written for this purpose (11). This program uses quadratic velocity-linear pressure elements within a mixed formulation of the steady equations: these elements are known to be stable and produce approximations of optimal order. The resulting nonlinear algebraic system is solved by a Newton-continuation method. Analytical gradients of the objective function are computed using a direct differentiation method.

#### Optimization strategy

The guiding procedure used to modify the design based on the evaluation of the objective function, i.e., to determine the "next move" in the design space can be selected from several families of available algorithms (12). Methods that do not explicitly require the gradient of the objective function or constraints, so-called "direct search" methods, were originally applied to this problem. These were later replaced by two different gradient-based methods that were found to be much more efficient: a method of feasible directions (13) and a sequential quadratic programming algorithm (12). Unlike direct search methods which rely on enumeration of the design space, these gradient-based algorithms require, and exploit, estimates of the local derivatives and curvatures of the design space, i.e., the "sensitivity" of the objective function to the design variables. Although these sensitivities are com-

monly obtained by finite differences, this approach would be far too time-consuming for shape optimization of complex shapes found in rotary pumps. Therefore, these design sensitivities were found by analytical differentiation of the flow equation at little additional cost beyond the flow simulation (11).

The outline of the overall shape optimization program is depicted schematically in Fig. 1. An initial geometry is provided to the CFD solver in parametric form. The resulting flow field is interpreted in terms of the objective functions, which in turn reflect the desired design criteria. If the optimal conditions are not satisfied, the design parameters are updated according to the optimization procedure, with the assistance of the design sensitivities. The process is repeated until an optimal geometry is reached.

#### Specific cases studied

Due to the difficulty of solving the large nonlinear optimization problem of a fully three-dimensional impeller pump, the shape optimization algorithm was initially applied to two simplified geometries: internal flow within a two-dimensional channel and external flow over a periodic blade cascade.

#### Two-dimensional flow channel

A representative flow path within a rotary blood pump involves the channeling of blood through a

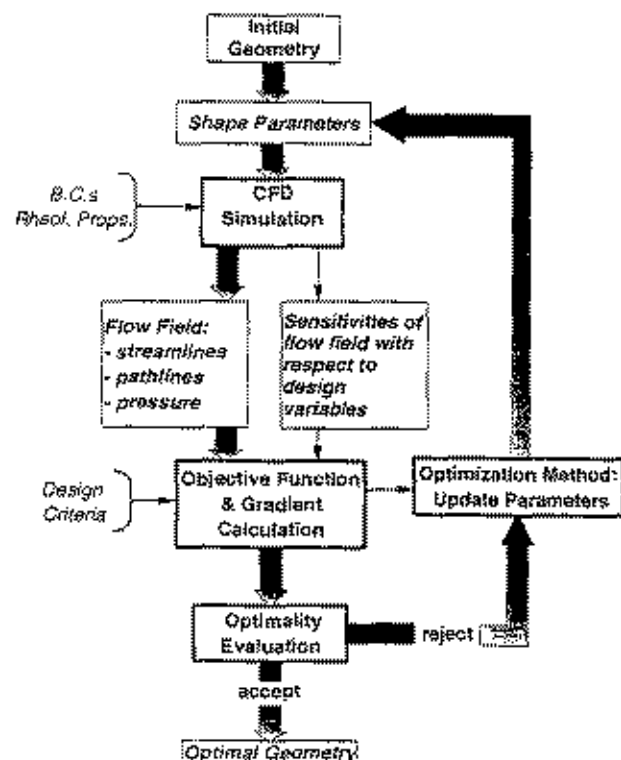


FIG. 1. A schema of the optimization methodology is shown.

prescribed angle. A simple example would be flow within the inlet or outlet cannulas. Such a flow geometry was modeled in this study by a constant-width turning passage. The centerline of the channel was parameterized in polar coordinates by a cosine series

$$r(\theta) = r_1 \cos(2\theta) + r_2 \cos(4\theta) + \dots \quad (4)$$

through a total angle of  $90^\circ$  with a total of 7 parameters. This domain was discretized by an unstructured mesh consisting of approximately 1,000 elements. The ends of this channel were allowed to an unstructured slide but were constrained to a maximum distance from the origin. A parabolic velocity distribution was assumed at the channel entrance with a mean velocity corresponding to a Reynolds number of 1,000. The exit was prescribed to be traction-free.

The coupled CFD-optimization program was implemented for this problem using a Digital 3000-400 (Alpha) workstation equipped with 128 Mb of memory. For each design iteration, the flow solution of the previous shape was used as an initial guess for the subsequent solution. All 6 available functions were tested independently for these simulations to evaluate the influence of objective function on the optimized geometry.

#### Stator blade cascade

A second series of optimization studies was conducted which considered the flow between a cascade of stator blades, or airfoils. This problem was chosen to represent the design task of selecting blade shape and separation (hence number of blades) to achieve the minimal viscous dissipation for a given flow deflection.

Due to the increased complexity of this geometry, a Bezier-Bernstein parameterization was adopted to describe the blade shapes (1), and the domain was discretized using an adaptive unstructured grid generator. The mesh nodes were clustered near the surface to better resolve viscous effects, such as boundary layers and separation points. A total of 16 shape parameters was used for this geometry, consisting of 14 Bezier control points and 2 additional parameter and the separation distance defining the stagger angle. The former essentially correspond to base profile and camberline of the blade shape whereas the latter provides control of the rigid body motion of the blades within the cascade.

It was assumed that the entrance flow distribution was uniform and inclined at an angle of  $45^\circ$ . The outflow was likewise uniform but horizontal with respect to the domain boundary. A periodic boundary condition was imposed to simulate an infinite,

or periodic, row of blades. An additional constraint was imposed to prevent the cross-sectional area of the blade from decreasing below 50% of its initial area.

The flow simulation used for this case experiment was performed at a Reynolds number of 141, and the entire optimization experiment was conducted on a Sun SPARCStation 10 workstation.

## RESULTS

### Flow channel

Several numerical optimization experiments were conducted with the flow channel to evaluate the effect of initial shape, number of design variables, end constraints, Reynolds number, and choice of objective function. The evolution of the geometry for the case of minimizing scaled viscous dissipation at a Reynolds number of 1,000 is shown in Fig. 2. The optimizer is observed to improve the initial shape by first increasing the radius of curvature of the bend then by fine tuning the parameters to smooth the flow profile. The poorly designed elbow was thus evolved toward a cardioid shape, having a larger radius at inflow with a gradually decreasing radius of curvature toward the outflow. The large recirculation bubbles and flow coarctation present in the initial elbow were virtually eliminated as a result. This representative case demonstrated a reduction in the viscous dissipation index of 68% (from 33.3 to 10.7) in relatively few (14) iterations. It was found that minimization of scaled viscous dissipation resulted in concomitant reductions in the subordinate objective functions, listed in Table I.

Comparison of the effect of objective function selection revealed that all three unscaled functions resulted in similar shapes. These shapes were different, however, from the area-scaled group. When minimizing any of the unscaled objectives, the optimizer tended to produce relatively straight passages with curved ends, favoring minimization of the area. By contrast, when seeking to optimize the scaled objectives, the optimizer expresses a preference to minimize the flow features primarily responsible for the flow disturbance, thus producing smoother shaped passages.

The total time required to perform these optimization procedures depended upon the optimization algorithm used and the particular conditions of the problem, such as the number of variables and constraints. Because of the efficiency of the coupled CFD-optimization algorithm employed, the average optimization run took approximately 4 h on the DEC Alpha workstation—only 16 times longer than the time required for a single CFD simulation.

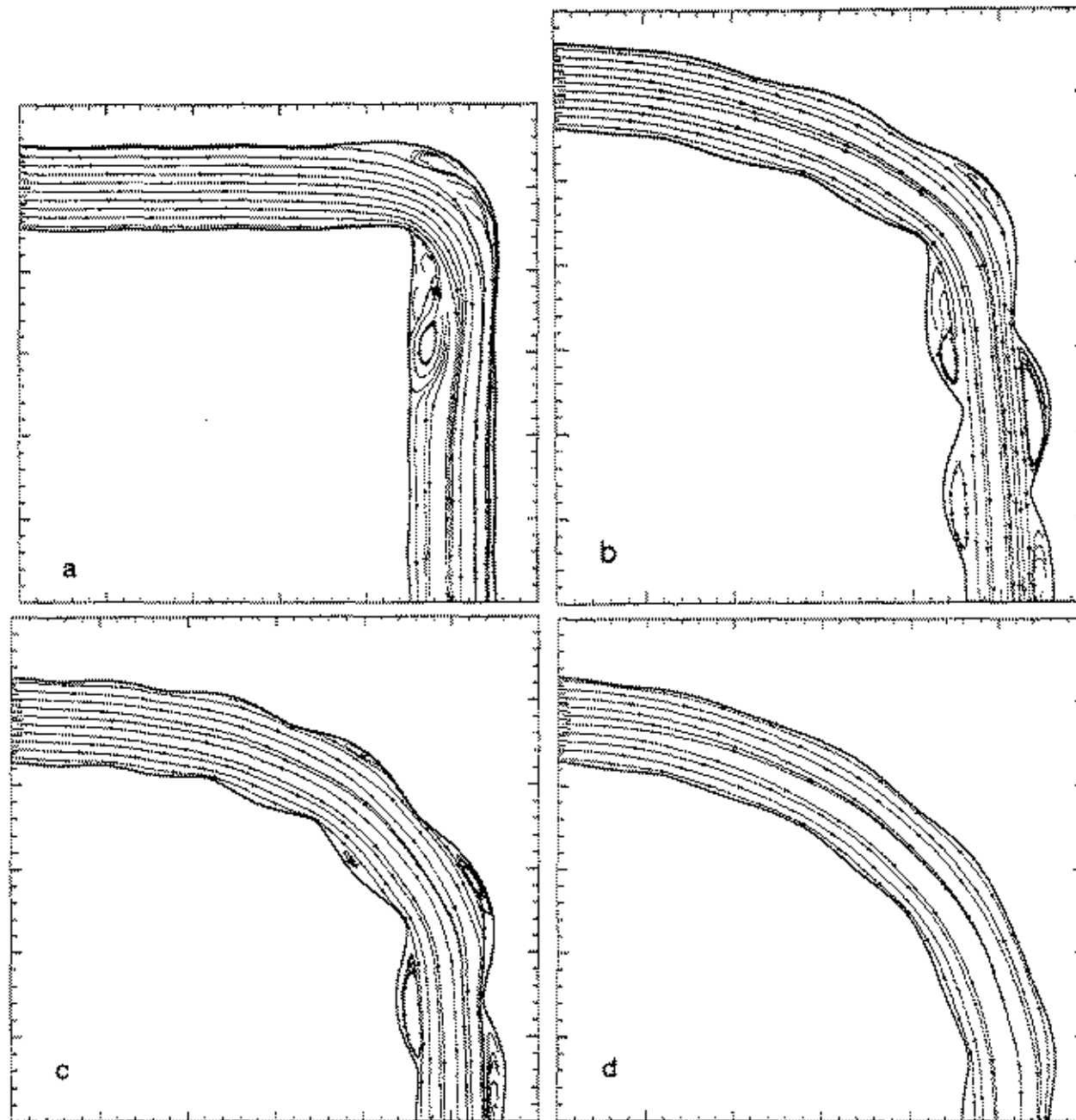


FIG. 2. The design evolution of a 90° channel is shown: initial a; shape; b,c; intermediate iterations. d: optimized shape. Li indicate particle traces.

#### Blade cascade

Figures 3a–c displays the initial, intermediate, and optimized shapes for the linear row of cascade blades. The flow-field computed about the initial blade design (a symmetric NACA-0012 profile) demonstrates strong velocity shear layers which envelop a large region of recirculation on the upper surface following the separation point at the leading edge. To maintain global mass continuity, a jet-like flow ensues in the midregion between the blades.

Within six iterations, the optimizer effected a dramatic improvement to the cascade flow by decreasing the blade separation-to-chord ratio, thinning blade profile, slightly turning the blades toward incident flow, and adding camber to the profile. The separation-to-chord ratio was altered over 3% (from 1.3 to 0.78) and was found to have the most dramatic effect upon the reduction of the flow separation and attendant viscous dissipation. Although the incident blade angle was expected to align m

## FLOW OPTIMIZATION OF BLOOD PUMP CASCADE

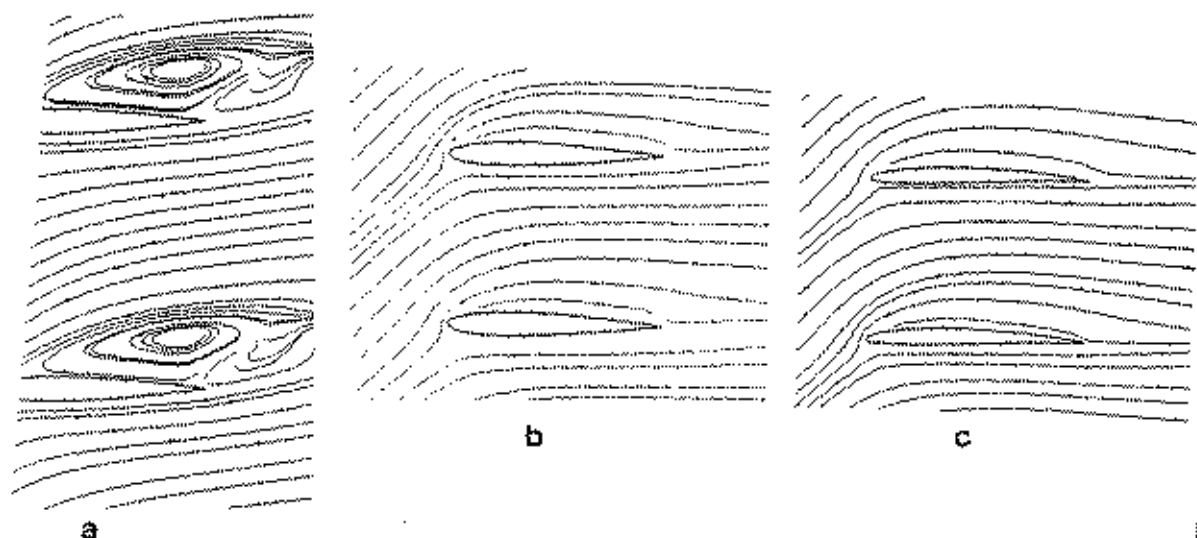


Fig. 1 Design evolution of the blade cascade is shown: a: initial guess (NACA-0012 airfoil); b: intermediate shape; c: final optimized shape

With the flow, a final stagger angle of  $-0.6^\circ$  was used to optimally satisfy the horizontal outflow constraint. The cross-sectional area of the cascade was reduced 35% in the final geometry. The increase in the area-scaled global viscous dissipation function (the objective function for this study) was 14% (from 6.9963 to 6.0063). The optimization required slightly under 1 h of computation on the Sun SPARCStation 10 workstation.

### DISCUSSION

In the pursuit of an optimum configuration of an axial blood pump involves the manipulation of numerous design parameters, arguably more than any human designer can manage at one time. These parameters include impeller speed, hub profile, rotor and stator geometry, chord/separation ratio (thus, number of blades), blade height, blade base profile, camberline, leading angle of incidence and deflection angle), clearance, and blade twist. Because of the strong coupling between the design criteria and perfor-

mance indices, it would be prohibitively costly and time-intensive to explore all the combinations and permutations of the possible design variables.

Traditional analysis methods, such as the Euler pump theory, may be able to provide partial insight into how some of these variables, such as blade deflection and rotor tip speed, affect performance (14,15). Unfortunately, these theories are not very useful in predicting how these variables will influence blood trauma. Indeed, experience has shown that many design parameters must be determined through an empirical parametric approach (3,16-18).

Recent advances in flow analysis tools, such as high-resolution flow visualization and computational fluid dynamics (CFD), offer an opportunity to reveal the underlying microflow features responsible for satisfactory performance and biocompatibility. Consequently, these tools are attracting increased attention in rotary blood pump analysis (19-23). Existing CFD software, however, still requires the designer to altering the design vari-

TABLE I. Objective function values for design optimization of  $90^\circ$  channel according to minimum viscous dissipation index,  $f_1$

Iteration	$f_1$	$f_2$	$f_3$	$f_4$	$f_5$	$f_6$
1	6.9963	0.0000	0.0000	0.0000	0.0000	0.0000
2	6.9963	0.0000	0.0000	0.0000	0.0000	0.0000
3	6.9963	0.0000	0.0000	0.0000	0.0000	0.0000
4	6.9963	0.0000	0.0000	0.0000	0.0000	0.0000
5	6.9963	0.0000	0.0000	0.0000	0.0000	0.0000
6	6.9963	0.0000	0.0000	0.0000	0.0000	0.0000
7	6.9963	0.0000	0.0000	0.0000	0.0000	0.0000
8	6.9963	0.0000	0.0000	0.0000	0.0000	0.0000
9	6.9963	0.0000	0.0000	0.0000	0.0000	0.0000
10	6.9963	0.0000	0.0000	0.0000	0.0000	0.0000
11	6.9963	0.0000	0.0000	0.0000	0.0000	0.0000
12	6.9963	0.0000	0.0000	0.0000	0.0000	0.0000
13	6.9963	0.0000	0.0000	0.0000	0.0000	0.0000
14	6.9963	0.0000	0.0000	0.0000	0.0000	0.0000
15	6.9963	0.0000	0.0000	0.0000	0.0000	0.0000
16	6.9963	0.0000	0.0000	0.0000	0.0000	0.0000
17	6.9963	0.0000	0.0000	0.0000	0.0000	0.0000
18	6.9963	0.0000	0.0000	0.0000	0.0000	0.0000
19	6.9963	0.0000	0.0000	0.0000	0.0000	0.0000
20	6.9963	0.0000	0.0000	0.0000	0.0000	0.0000
21	6.9963	0.0000	0.0000	0.0000	0.0000	0.0000
22	6.9963	0.0000	0.0000	0.0000	0.0000	0.0000
23	6.9963	0.0000	0.0000	0.0000	0.0000	0.0000
24	6.9963	0.0000	0.0000	0.0000	0.0000	0.0000
25	6.9963	0.0000	0.0000	0.0000	0.0000	0.0000
26	6.9963	0.0000	0.0000	0.0000	0.0000	0.0000
27	6.9963	0.0000	0.0000	0.0000	0.0000	0.0000
28	6.9963	0.0000	0.0000	0.0000	0.0000	0.0000
29	6.9963	0.0000	0.0000	0.0000	0.0000	0.0000
30	6.9963	0.0000	0.0000	0.0000	0.0000	0.0000
31	6.9963	0.0000	0.0000	0.0000	0.0000	0.0000
32	6.9963	0.0000	0.0000	0.0000	0.0000	0.0000
33	6.9963	0.0000	0.0000	0.0000	0.0000	0.0000
34	6.9963	0.0000	0.0000	0.0000	0.0000	0.0000
35	6.9963	0.0000	0.0000	0.0000	0.0000	0.0000
36	6.9963	0.0000	0.0000	0.0000	0.0000	0.0000
37	6.9963	0.0000	0.0000	0.0000	0.0000	0.0000
38	6.9963	0.0000	0.0000	0.0000	0.0000	0.0000
39	6.9963	0.0000	0.0000	0.0000	0.0000	0.0000
40	6.9963	0.0000	0.0000	0.0000	0.0000	0.0000
41	6.9963	0.0000	0.0000	0.0000	0.0000	0.0000
42	6.9963	0.0000	0.0000	0.0000	0.0000	0.0000
43	6.9963	0.0000	0.0000	0.0000	0.0000	0.0000
44	6.9963	0.0000	0.0000	0.0000	0.0000	0.0000
45	6.9963	0.0000	0.0000	0.0000	0.0000	0.0000
46	6.9963	0.0000	0.0000	0.0000	0.0000	0.0000
47	6.9963	0.0000	0.0000	0.0000	0.0000	0.0000
48	6.9963	0.0000	0.0000	0.0000	0.0000	0.0000
49	6.9963	0.0000	0.0000	0.0000	0.0000	0.0000
50	6.9963	0.0000	0.0000	0.0000	0.0000	0.0000
51	6.9963	0.0000	0.0000	0.0000	0.0000	0.0000
52	6.9963	0.0000	0.0000	0.0000	0.0000	0.0000
53	6.9963	0.0000	0.0000	0.0000	0.0000	0.0000
54	6.9963	0.0000	0.0000	0.0000	0.0000	0.0000
55	6.9963	0.0000	0.0000	0.0000	0.0000	0.0000
56	6.9963	0.0000	0.0000	0.0000	0.0000	0.0000
57	6.9963	0.0000	0.0000	0.0000	0.0000	0.0000
58	6.9963	0.0000	0.0000	0.0000	0.0000	0.0000
59	6.9963	0.0000	0.0000	0.0000	0.0000	0.0000
60	6.9963	0.0000	0.0000	0.0000	0.0000	0.0000
61	6.9963	0.0000	0.0000	0.0000	0.0000	0.0000
62	6.9963	0.0000	0.0000	0.0000	0.0000	0.0000
63	6.9963	0.0000	0.0000	0.0000	0.0000	0.0000
64	6.9963	0.0000	0.0000	0.0000	0.0000	0.0000
65	6.9963	0.0000	0.0000	0.0000	0.0000	0.0000
66	6.9963	0.0000	0.0000	0.0000	0.0000	0.0000
67	6.9963	0.0000	0.0000	0.0000	0.0000	0.0000
68	6.9963	0.0000	0.0000	0.0000	0.0000	0.0000
69	6.9963	0.0000	0.0000	0.0000	0.0000	0.0000
70	6.9963	0.0000	0.0000	0.0000	0.0000	0.0000
71	6.9963	0.0000	0.0000	0.0000	0.0000	0.0000
72	6.9963	0.0000	0.0000	0.0000	0.0000	0.0000
73	6.9963	0.0000	0.0000	0.0000	0.0000	0.0000
74	6.9963	0.0000	0.0000	0.0000	0.0000	0.0000
75	6.9963	0.0000	0.0000	0.0000	0.0000	0.0000
76	6.9963	0.0000	0.0000	0.0000	0.0000	0.0000
77	6.9963	0.0000	0.0000	0.0000	0.0000	0.0000
78	6.9963	0.0000	0.0000	0.0000	0.0000	0.0000
79	6.9963	0.0000	0.0000	0.0000	0.0000	0.0000
80	6.9963	0.0000	0.0000	0.0000	0.0000	0.0000
81	6.9963	0.0000	0.0000	0.0000	0.0000	0.0000
82	6.9963	0.0000	0.0000	0.0000	0.0000	0.0000
83	6.9963	0.0000	0.0000	0.0000	0.0000	0.0000
84	6.9963	0.0000	0.0000	0.0000	0.0000	0.0000
85	6.9963	0.0000	0.0000	0.0000	0.0000	0.0000
86	6.9963	0.0000	0.0000	0.0000	0.0000	0.0000
87	6.9963	0.0000	0.0000	0.0000	0.0000	0.0000
88	6.9963	0.0000	0.0000	0.0000	0.0000	0.0000
89	6.9963	0.0000	0.0000	0.0000	0.0000	0.0000
90	6.9963	0.0000	0.0000	0.0000	0.0000	0.0000
91	6.9963	0.0000	0.0000	0.0000	0.0000	0.0000
92	6.9963	0.0000	0.0000	0.0000	0.0000	0.0000
93	6.9963	0.0000	0.0000	0.0000	0.0000	0.0000
94	6.9963	0.0000	0.0000	0.0000	0.0000	0.0000
95	6.9963	0.0000	0.0000	0.0000	0.0000	0.0000
96	6.9963	0.0000	0.0000	0.0000	0.0000	0.0000
97	6.9963	0.0000	0.0000	0.0000	0.0000	0.0000
98	6.9963	0.0000	0.0000	0.0000	0.0000	0.0000
99	6.9963	0.0000	0.0000	0.0000	0.0000	0.0000
100	6.9963	0.0000	0.0000	0.0000	0.0000	0.0000

manually, trading between competitive objectives. In other words, CFD analysis alone cannot make design decisions and cannot execute the necessary design modifications required to alleviate undesirable flow conditions.

The algorithm described in the current paper represents an attempt to improve the utility of CFD analysis in the design process. By coupling the versatility of CFD with efficient optimization methods, it has become possible to revise automatically the design variables according to specified criteria of the predicted flow. This allows the design process to be initiated with a conceptual flow path, motivated by intuition or first-order analysis, for example. The CFD-optimizer will then evolve this initial design—based on the fluid dynamic characteristics relevant to blood trauma.

Despite the simplifications made in the test problems studied, these problems retain many of the features and the mathematical structure as the general problem, thus providing insight into solution properties, sensitivity of the optimum to various problem data, influence of different objective functions, performance of algorithms, etc. The results obtained with the turning channel problem successfully demonstrated the fundamental capabilities of the shape optimization algorithm to evolve a superior, flow-optimized, blood path from an initially poor original design. In all channel cases studied, the inferior initial shape was rapidly modified to reduce the level of dissipation, vorticity, and shear. While the optimizer often converged upon geometries that were predicted intuitively, in some cases unexpected results were generated. This demonstrated the ability of the optimizer to strike a balance between competing design objectives, such as minimum area versus minimum shear.

The converged optimum design depends upon the objective function specified to the optimizer. The ultimate objective in blood pump design is to maximize performance while avoiding flow conditions leading to blood trauma and deposition. In an attempt to interpret these criteria in terms of the fluid dynamics, several candidate objective functions were independently studied. Although not exhaustive, these results demonstrated that relatively "smooth" flow patterns could be achieved by minimizing any of the objective functions studied: viscous dissipation, vorticity, or shear. Normalizing these objectives with respect to area resulted in more favorable optimized shapes.

The stator blade cascade optimization experiment, although simplified to two dimensions, provides insight toward the ubiquitous problem of se-

lecting blade spacing and number. As the number of blades increases, and the separation/chord ratio decreases, more guidance is given to the flow. Thus the likelihood for flow separation is reduced. At the same time, however, more blades result in increased skin friction. The optimum choice of blade number, therefore, would be that which balances these two contending design goals. By minimizing viscous dissipation, the numerical optimization algorithm was able to achieve this balance, resulting in virtual elimination of boundary layer separation. Consequently, the likelihood for cell trauma and blood element deposition will be dramatically reduced.

When considering the computational flow optimization of a complete blood pump, additional objective functions will become increasingly important, such as overall size, hydrodynamic (H-Q) performance, power consumption, etc. Further constraints will also have to be factored into the design problems, such as manufacturability, structural integrity, rotordynamics, etc. Additional fluid dynamic criteria will also be explored, including indices of flow reversal and adverse pressure gradient leading, for example, to cavitation and separation. Experimental validation studies under way will help estimate the error associated with the assumptions and simplifications introduced in the current model and will suggest areas of improvement for further refinement. The utility and performance of this algorithm will also benefit from future improvements in hemorrheological modeling, such as cell trauma criteria that account for time-varying shear history and constitutive models that incorporate non-Newtonian effects of shear thinning, viscoelasticity, and anisotropy.

The major challenges in extrapolating the current methodology to three dimensions are in the parameterization of three-dimensional shapes, such as impellers and volutes, and in the accommodation of the large-scale nature of the optimization problem. It is anticipated that the former will be addressed through the application of parametric constructive solid geometry software. The steadily increasing computer power and availability of massively parallel supercomputers provides promise for attaining the latter goal (24).

It is hoped that the application of automated CFD optimization to rotary blood pump design will allow increased attention to microflow criteria earlier in the design cycle—not only for achieving satisfactory results, but also for saving time and expense associated with making changes downstream in the design process.



**Acknowledgments:** The authors wish to express their gratitude to the McGowan Foundation for their beneficence in supporting this research. Also, the authors thank Mr. Sean Kowalski for his skillful computer support which was instrumental in completing these studies. INDNJC.

## REFERENCES

- Burgreen GW. Three-dimensional aerodynamic shape optimization of using discrete sensitivity analysis. PhD dissertation, Old Dominion University, Norfolk, Virginia, 1994.
- Huddleson DH. Aerodynamic design optimization using computational fluid dynamics. PhD Dissertation, University of Tennessee, Knoxville, 1989.
- Schima H, Muller MR, Papanonis D, Schlusche C, Huber L, Schmidt C, Trubei W, Thoma H, Losert U, Wolner E. Minimization of hemolysis in centrifugal blood pumps: influence of different geometries. *Int J Artif Organs* 1992;16(17):521-9.
- Leverett LB, Hellums JD, Alfrey CP, Lynch EC. Red blood cell damage by shear stress. *Biophysical J* 1972;12:257-73.
- Blackshear PL. Mechanical hemolysis in flowing blood. In: Fung YC, Perrone N, Anliker M, eds. *Biomechanics—its foundations and Objectives*. Englewood Cliffs: Prentice-Hall, 1972:501-28.
- Heuser G, Optiz R. A Couette viscometer for short time shearing of blood. *Biorheology* 1980;17:17-24.
- Einav S, Reul H, Rau G, Elad D. Shear stress blood damage along the cusp of a tri-leaflet prosthetic valve. *Artif Organs* 1991;14:716-20.
- Schistek R. Various designs of nonpulsatile blood pumps. In: Unger F, ed. *Assisted circulation 3*. Berlin: Springer Verlag, 1989:233-42.
- Wagner WR, Johnson PC, Kormos RL, Griffith BP. Evaluation of bioprosthetic valve-associated thrombus in ventricular assist device patients. *Circulation* 1993;2023-9.
- Leonard EF. Principles of cardiovascular device design. *Cardiovasc Pathol* 2 (3 Suppl):3s-10s.
- He B, Ghattas O, Antaki JF, Dennis YJ. Shape optimization of Navier-Stokes flows with application to optimal design of artificial heart components. In: *5th AIAA/USAF/NASA/ISSMO Symposium on Multidisciplinary Analysis and Optimization*, Panama City Beach, FL, September 7-9, 1994, pp. 1202-12.
- Gill P, Murray W, Wright M. *Practical optimization*. New York: Academic Press, 1981.
- Vanderplaat GN, Moses F. *Structural optimization by methods of feasible directions*. Computers and Structures. Vol. 3., 1973:739-55.
- Qian K. Haemodynamic approach to reducing thrombosis and haemolysis in an impeller pump. *J Biomed Eng* 1990;12:533-5.
- Rathod MS. Theoretical analysis and design of a centrifugal blood pump for optimum blade number and angle. PhD Dissertation, Mississippi State University, 1975.
- Mizuguchi K, Damm GA, Bozeman RJ, Akkerman JW, Aber GS, Svejtkovsky PA, Takatani S, Nosé Y, Noon GP, DeBakey ME. Development of the Baylor/NASA axial flow pump: in vitro performance and hemolysis test results. *Artif Organs* 1994;18:32-43.
- Ohara Y, Makinouchi K, Orime Y, Tsai K, Naito K, Mizuguchi K, Shimono K, Damm G, Glueck J, Takatani S, Noon GP, Nosé Y. An ultimate, compact, seal-less centrifugal ventricular assist device: Baylor c-gyro pump. *Artif Organs* 1994;18:17-4.
- Yamazaki K, Umezumi M, Koyanagi H, Kitamura M, Eisbi K, Kawai A, Tagusari O, Niinami H, Akimoto T, Nojiri C, Tsuchiya K, Mori T, Iiyama H, Endo M. A miniature intra-ventricular axial flow blood pump that is introduced through the left ventricular apex. *ASAIO J* 1992;M679-83.
- Papanonis DE. Numerical prediction of the shear stresses and the mean stay time for radial flow impellers. In: Schima H, Thoma H, Wieselthaler G, Wolner E (eds). *Proceedings of the International Workshop on Rotary Blood Pumps* 1991:63-69.
- Kiris C. Incompressible viscous flow computations for the pump components of the artificial heart. *MCAT Institute Report* 92-003, March 1992.
- Biadyszewicz C, Gaylor JDS. Numerical calculation of flow behaviour within centrifugal blood pumps (CBP). In: *Proceedings of The American Society of Artificial Internal Organs 39th Annual Meeting*, 1993:42.
- Treichler J, Rosenow SE, Damm G, Naito K, Ohara Y, Mizuguchi K, Makinouchi K, Takatani S, Nosé Y. A fluid dynamic analysis of a rotary blood pump for design improvement. *Artif Organs* 1993;17:797-808.
- Kerrigan JP, Antaki JF, Maher TR, Shaffer FD. Quantitative measurement of steady flow patterns in a miniature axial flow blood pump using fluorescent image tracking velocimetry. In: *Proceedings of ASME Fluids Engineering Division Summer Meeting*, June 19-23, 1994:155-60.
- Orozco CE, Ghattas ON. Massively parallel aerodynamic shape optimization. *Computing Sys Eng* 1992;1-6:311-20.